Effects of Weld Discontinuities on Fatigue Strength of Laser Beam Welds

This study demonstrates that computational modeling is a useful tool in understanding weld discontinuity-fatigue property relationships.

BY P. -C. WANG AND S. DAVIDSON

ABSTRACT. The effects of weld discontinuities (*i.e.*, weld underfill, poor joint clearance and insufficient root penetration) on fatigue strength of lap joint laser beam welds have been investigated. Fatigue testing of laser beam welds with weld discontinuities were conducted. A fatigue prediction model that takes into account weld geometry changes and a statistical analysis method were both employed to evaluate the separate effects of these discontinuities on fatigue resistance. It was found that within the dimension range studied here, inadequate root penetration and/or poor joint clearance substantially decreased the fatigue life. The presence of underfill degraded the fatigue properties, and the decrease is more pronounced as the gauge is increased. The relative importance of weld discontinuities on fatigue life is ranked in decreasing order as follows: inadequate root penetration, poor joint clearance and weld underfill.

Introduction

Recent trends toward economically fabricating vehicle structures while ensuring quality have led to the implementation of laser beam welding (LBW) in the automobile industry. It has been shown to offer higher speed, greater precision and flexibility when compared with spot welding. While a great deal of effort has been focused on developing processing systems, there is an urgent need to understand the effects of weld discontinuities (*i.e.*, poor joint clearance, weld underfill and incomplete root penetration) on the durability of laser-welded components.

A common problem in LBW of automotive sheet steels, especially galvanized, is the presence of weld discontinuities. An underfill (Fig. 1A) is defined as a depression on the weld bead surface extending below the adjacent surface of the base metal. It can be deep or shallow, and it can have a ridge in the middle (Fig. 1B and C) depending on the process parameters (Ref. 1). Joint clearance refers to the distance between the faying surfaces of a joint — Fig. 1. Root penetration refers to the distance that the weld metal extends into the joint root (Ref. 2). Although the base metal composition influences the propensity toward discontinuity formation, the primary cause arises from incorrect welding speed, shielding gas pressure and welding power or tool conditions, and consequently lead to formation of discontinuities. Since there are many processing parameters to control under the production environment, it is conceivable that welded components may contain some weld discontinuities. Under service loading conditions, these weld discontinuities may induce stress concentrations and therefore result in fatigue crack initiation and propagation. It is essential that an understanding of the effects of weld discontinuities on fatigue resistance of laser beam welds be obtained.

KEY WORDS

Bead Width
Crack Propagation
Discontinuities
Fatigue Life
Finite Element Model
Interfacial Gap
Laser Beam Welding
Steel Sheet
Underfill
Weld Parameters

A difficulty arises when evaluating weld discontinuity effects in that underfill, joint clearance and root penetration are interrelated. For example, changes in underfill are often accompanied by changes in joint clearance and root penetration. It is not easy to alter one without changing the others. It is apparent that to experimentally separate the individual effects of underfill, joint clearance and root penetration is nearly impossible. The present study was undertaken to experimentally and analytically evaluate the individual effects of underfill, joint clearance and root penetration.

Lap joint laser beam welds were made from 0.76-mm (0.03-in.) and 1.83-mm (0.072-in.) gauge low-carbon sheet steels in which ranges of underfills, joint clearances and root penetration typically found in laser beam welded prototype components were prepared. To determine the relationship between underfill, joint clearance and root penetration, laser weld cross-sections were examined. Welded specimens were subjected to a zero-to-tensile cyclic load (R = 0, where R = min/max load). A fatigue model and a statistical analysis method were employed to separate the individual effects of the three types of weld discontinuities. Finally, results from the fatigue model were compared with experimental data to verify the accuracy of the model.

J-Integral Model

There are three approaches to fatigue modeling of thin gauge automotive weldments. They are: remote loads and stresses, weld local strains and stresses (Refs. 3, 4) and fracture mechanics parameters (Refs. 5–8). In this paper, a frac-

P. -C. WANG is with the Physics Department, General Motors Research Laboratories, Warren, Mich. S. DAVIDSON is with the University of Michigan.

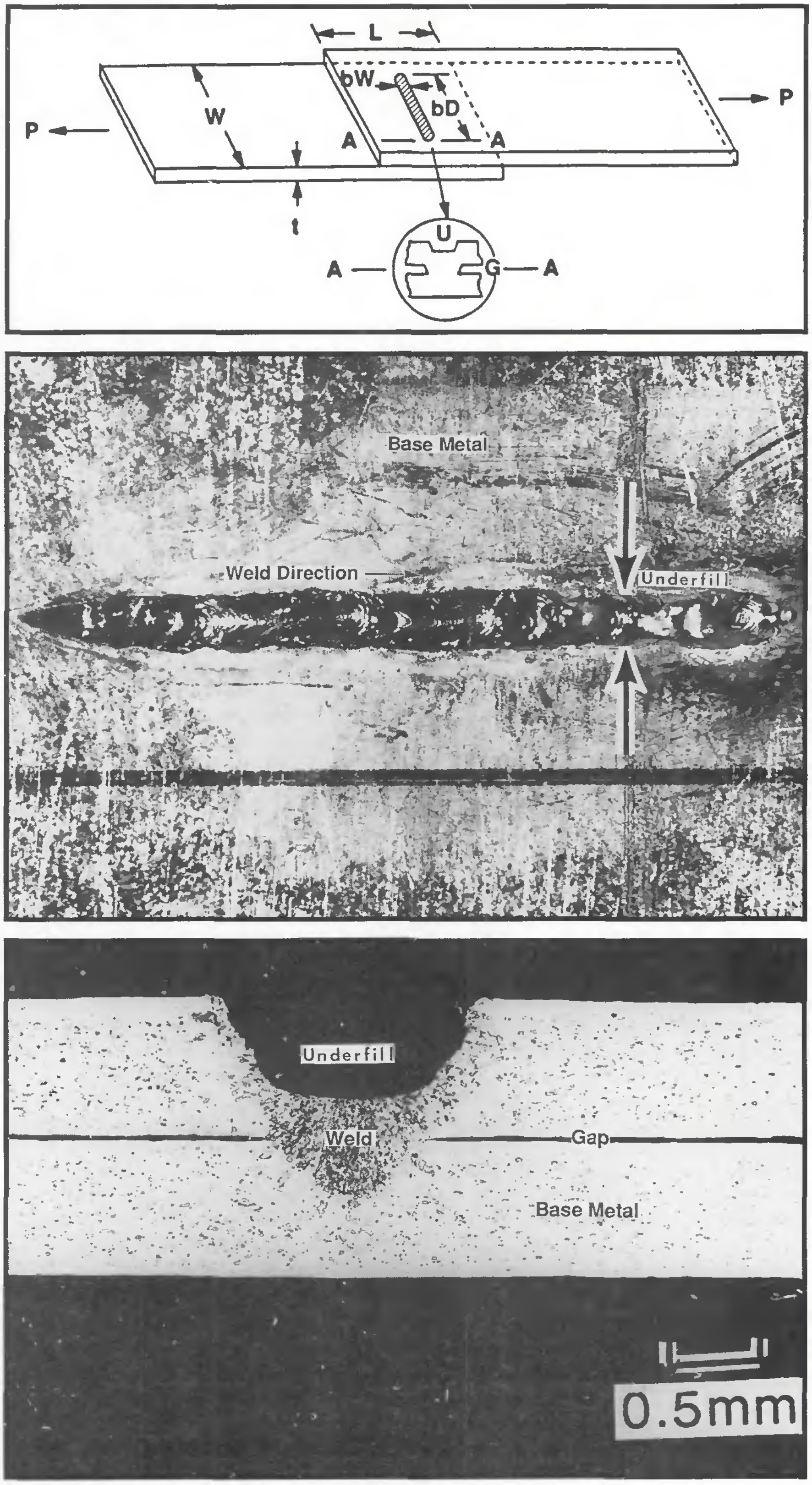

Fig. 1 — A — Schematic of a laser beam weld; B — photograph of a laser beam weld; C — cross-section at the arrow location shown in B.

ture mechanics approach is used to model the fatigue life of laser beam welds. A fracture mechanics parameter, J-integral, is employed to derive an equation relating experimental data with J-integral value. To simplify the model development process, it is subdivided into three phases: 1) fatigue test data generation, 2) finite element J-integral calculation, and 3) correlation of fatigue test results with J-integral. Each step is briefly described below.

Fatigue Data Generation

Table 1 lists the dimensions for seven groups of laser beam welds used in model development. Fatigue test results for these laser beam welds are plotted in Fig. 2. A regression analysis was used to determine load vs. life curves for each weld. Note that the fatigue life of Weld G is much higher than that for Weld A. Fatigue life at a given value of load can exhibit a difference of more than one order of magnitude. The life difference is much larger than the data scatter within each group. The data suggest that fatigue life is strongly dependent on specimen geometry.

J-Integral Calculation

Definition of J-Integral

The definition of the J-integral, as given by Rice (Ref. 9), is

$$J = \int_\Gamma W\,dY\ T\frac{\partial u}{\partial x}\,ds$$

where Γ is an arbitrary counterclockwise contour enclosing the notch tip of Fig. 3, ds is an element of arc length along Γ, W is the strain energy density ($W = \int \sigma_{ij} d\varepsilon_{ij}$, where σ_{ij} and ε_{ij} are the stress tensor and strain tensor, respectively), T is the traction vector associated with the outward normal n to T, and u is the displacement vector. The integral can be carried out using a finite element method.

Finite Element Model

The laser welds shown in Fig. 1 join two steel coupons with thickness t and width W. A generalized weld bead, which is perpendicular to the applied load P, is assumed with bead width bW and bead length bD. The steel coupons are overlapped by a distance L. A joint clearance is represented by G. Figure 4 shows the element grids for half of a laser beam weld. The weld is uniformly loaded across the two ends of the specimen. Since the loading axis is a line of symmetry, only half of the weld is analyzed. A notch exists at the junction of unwelded and welded regions at the faying surfaces of the specimen. The three-dimensional elements selected are 20-node brick and 20-node singular elements. Singular elements are used around the notch front and 20-node brick elements are used everywhere else. The singular elements have a square-root singular stress field at the notchfront (Ref. 10). As shown in Fig. 4, the start and end of the weld bead are represented by semicircles, which is the typical shape observed in the test specimens, with a radius equal to half of the bead width. The notchfront along the weld bead is represented by a wedge-shaped slot of 45 deg, which is confirmed from cross-sectional examinations. Weld underfill is modeled by a smooth saddle — Fig. 4. Although this is not typically observed in the laser beam welds, nevertheless, it can provide conservative estimations.

The finite element grid in Fig. 4 has 2662 nodes and 448 elements. The material is assumed to be linear elastic. Young's modulus and Poisson's ratio of the steel are 2.05 X 10^5 MPa (3.0 X 10^4 ksi) and 0.3, respectively. All calculations are performed with the ABAQUS code (Ref. 11) on a Cray computer.

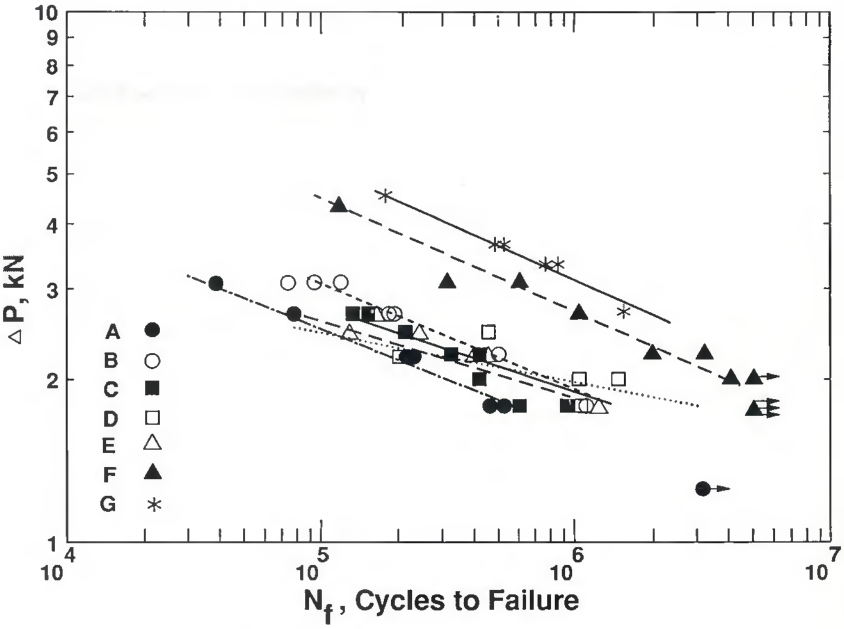

Fig. 2 — Fatigue test results for seven different laser beam welds.

J-Integral Value

The J values along the periphery of a laser beam weld with dimensions t = 0.76 mm (0.03 in.), W = 38.1 mm (1.5 in.), L = 38.1 mm, bW = 1.2 mm (0.05 in.), bD = 25.4 mm (1.0 in.) and G = 10% is computed and shown in Fig. 5 for a load P of 2.1 kN (470 lb). The degree of joint clearance, expressed in %, is defined as the sheet separation divided by the single coupon thickness. As shown, J has a value of 0.04 kJ/m^2 (1 kJ/m^2 = 68.52 ft-lb/ft^2) at the center, and reaches its peak value of 0.35 kJ/m^2 at the tip of the weld bead. These results imply that branch cracks will occur at the start or end of the weld bead.

Correlation of J-Integral Value with Fatigue Test Data

In a fatigue situation where crack propagation is dominant, fatigue life can be estimated by integrating the stress intensity range, ΔK, from an initial crack size to final size, where $\Delta K = K_{max} - K_{min}$. However, crack shapes are complex and change as cracks propagate. It is difficult to estimate stress intensity so-

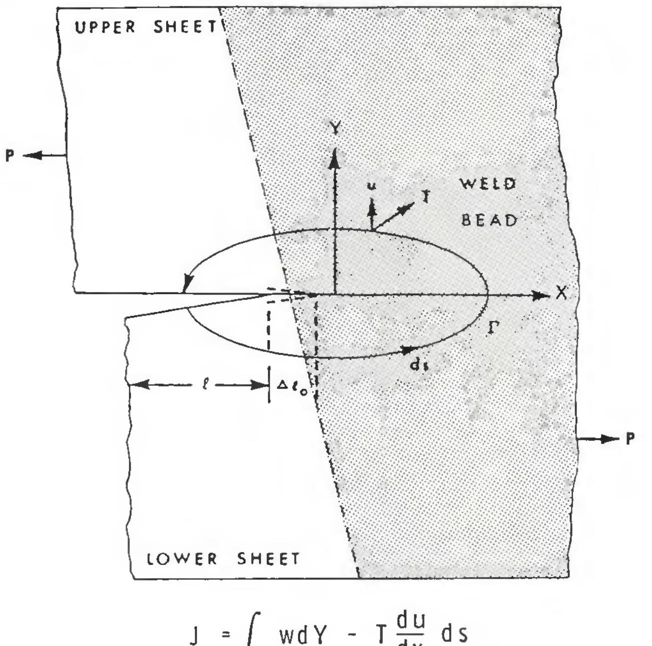

$$J = \int_{\Gamma} w dY - T \frac{du}{dx} ds$$

Fig. 3 — Notch-tip coordinate systems and arbitrary line integral contour.

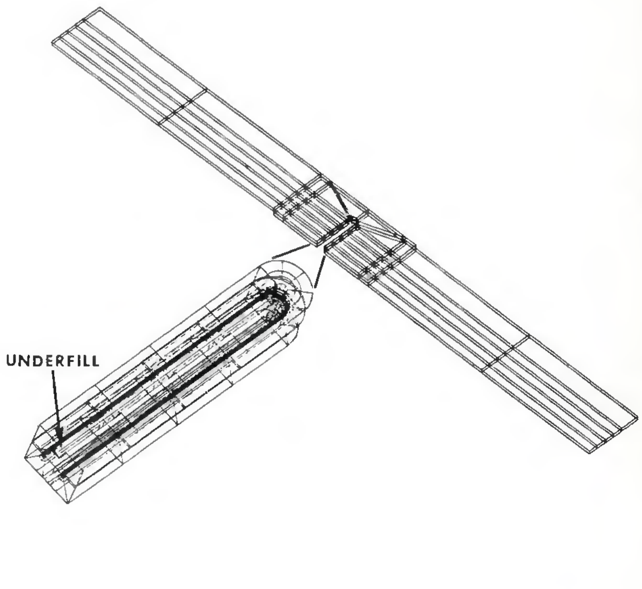

Fig. 4 — Finite element mesh for the laser beam weld. The inset drawings show the detail of the finite element modeling at the notch front and weld bead.

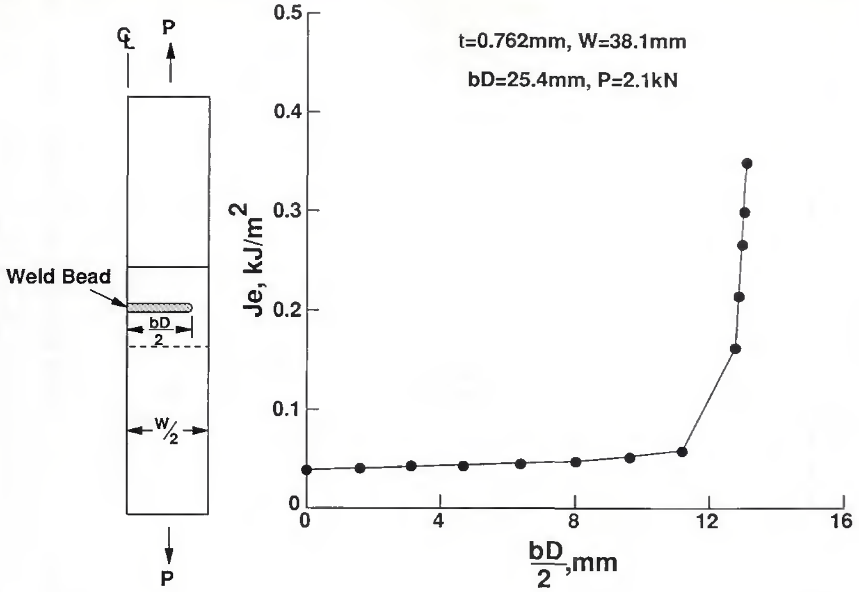

Fig. 5 — Left — Schematic sketch for half of the laser beam weld; right— variation of J-integral values with the periphery of the weld bead.

lutions at various crack lengths for a laser beam weld. Therefore, it is impractical to use the above approach. Instead, we will use the maximum initial J-integral value as a measure of the propensity for crack advance in a given weld geometry.

ΔJ ($\Delta J = J_{max} - J_{min}$, where J_{max} is calculated at the maximum load and J_{min} is calculated at the minimum load) values at various load levels for the seven welds included in Table 1 are computed. They are plotted against fatigue lives N_f in Fig. 6. For each data point, the abscissa is the experimental fatigue life data and the ordinate is the ΔJ value calculated from the applied load range, weld geometry and material properties. A least squares fit through these data points gives the following equation:

$$N_f = 3.5 \times 10^4 (\Delta J)^{-2.33} \qquad (2)$$

where N_f is in cycles and (ΔJ) is in kJ/m². The correlation coefficient is 0.79. As shown in Fig. 6, at a given ΔJ value, the scatter in life is within a factor of two. In comparison to the load vs. life plot shown in Fig. 2, where the fatigue lives for the seven weld geometries do not always overlap, using the ΔJ parameter collapses the fatigue data of different laser welded geometries into a narrow band. The ΔJ parameter allows designers to estimate the fatigue life of laser beam welds without having to resort to extensive test programs.

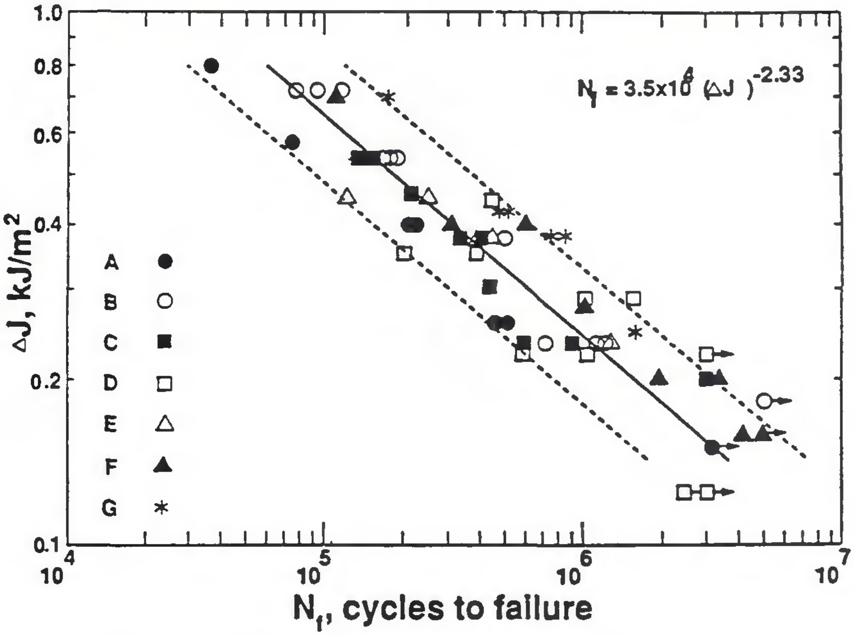

Fig. 6 — Correlation of J-integral value with the fatigue life of laser beam welds.

Experimental Procedure

Specimen Preparation

Bare SAE 1005 AK sheet steel with gauges of 0.76 mm (0.03 in.) and 1.83 mm (0.072 in.) were used. The laser beam welds were fabricated from 38.1 X 127-mm (1.5 X 5-in.) coupons sheared from sheets with the longer dimension parallel to the rolling direction. A 25.4-mm (1-in.) long laser beam weld was centered on the 25.4-mm overlap region.

To study the underfill effect, welds with three underfills of 0, 24 and 50% were prepared by adjusting the joint clearance between the sheets. A fixture was used to achieve the desired joint clearance. The percent underfill, which is used to describe the degree of the underfill, is defined as the deepest depression on the weld surface divided by the single coupon thickness. The coupons were welded with a Spectra-Physics (Rofin-Sinar) Model 825 carbon dioxide laser (2.75 kW). Coupons were fixed on a movable, motor-driven table whose velocity was controlled. The welds were made by moving the workpiece on the table under a stationary laser system. Table 2 lists the LBW parameters that gave the best results based on weld bead appearance and/or completeness of penetration.

Underfill Profile Measurement

Optical measurements were taken along the weld centerline using a microscope with a calibrated focus knob. Each reading represents the highest (or lowest) value at 1-mm (0.04-in.) intervals along the weld bead. For each point, the foundation (sheet surface) was determined by averaging two measurements at the right and left sides of the weld bead. Then, the difference between the readings along the weld centerline and the foundation is plotted as a point on the weld profile. The accuracy of the absolute underfill values is estimated to be about 1.5%, due mainly to error in image focusing.

Cross-Section Examinations

To determine the relationship between joint clearance and root penetration, cross-sections of six specimens with various underfills were examined.

Each specimen was sectioned along the loading direction to obtain sections perpendicular to the weld. Three sections (start, middle and end of the weld) were taken from each specimen. Photographs were taken by a low-power binocular microscope using oblique illumination.

Fatigue Testing

Specimens were gripped in self-aligning hydraulic grips and then cycled in an Instron machine (Model 1331) under ambient laboratory conditions from zero to a tensile load ($R = 0$, where R = min/max load). To minimize bending stresses during testing, both ends of the specimens were attached by adhesive to two filler plates of the same thickness. All fatigue tests were performed at 10–20-Hz frequency. Tests were terminated when specimen separation occurred through weld bead failure. If a specimen did not fail, a test was terminated at about three- to five-million cycles.

Experimental Results

Underfill Profile Measurement

Figure 7 A–B shows the surface appearances of 1.83-mm gauge specimens with 50% underfill. As shown, there are depressions and ridges on the weld surface. Underfill profile along the weld centerline is shown in Fig. 7C. Underfill varies along the weld bead, and a big dimple is seen at about 5 mm (0.2 in.) away from the end of the weld. This is mainly caused by existence of molten metal flowing into the sheet separation during LBW. A 50% underfill is obtained by dividing the deepest depression along the weld bead by the steel thickness. Similar results were also observed for the case of 0.76-mm specimens.

Table 1 — Dimensions of Lap Laser Beam Welds

Specimen	Sheet Thickness (mm)	Bead Length (mm)	Bead Width (mm)	Joint Clearance (%)	Overlap (mm)
A	0.76	25.4	1.2	10	38.1
B	0.76	25.4	1.2	10	38.1
C	0.76	25.4	1.2	0	38.1
D	0.76	25.4	1.2	0	38.1
E	0.76	25.4	1.2	10	38.1
F	1.78	25.4	1.2	0	25.4
G	1.78	25.4	1.4	14	25.4

Table 2 — Laser Beam Welding Parameters

Sheet Thickness (mm)	Welding Power (kW)	Welding Speed Gas (cm/min)	Shielding Gas	Shielding Flow (m^3/h)	Focal Length (mm)	Beam Diameter (mm)	Beam Mode
0.76	2.6	267	He	0.85	190	0.76	TEM_{20}
1.83	2.6	127	He	0.85	190	0.76	TEM_{20}

Cross-Section Examinations

Because the underfill varies along the weld bead, three cross-sections (*i.e.*, weld start, middle and end) for each specimen were prepared. Visual and optical examinations of specimens showed that the greater the root penetration, the larger is the weld bead width. Thus, bead width was utilized in the remainder of this paper to represent root penetration. For each cross-section, the bead width and joint clearance near the weld bead were measured. The average bead width is plotted against average joint clearance in Fig. 8 for 0.76-mm and 1.83-mm gauge welds. In this figure, each point represents the average of three measurements. Fitting the data to a straight line, using a least-squares regression analysis, gives

$$bW \text{ (bead width)} = 0.81\ (G) + 0.77 \text{ for 0.76-mm gauge} \quad (3)$$

$$bW \text{ (bead width)} = 1.07\ (G) + 0.98 \text{ for 1.83-mm gauge} \quad (4)$$

where bW is in mm. The associated correlation coefficients are $r = 0.33$ and 0.66 for 0.76- and 1.83-mm gauge, respectively; thus reflecting the large data scatter. Student t test for small sample sizes (Ref. 12) reveals that there is a significant difference between the mean values of the bead width for a small and large joint clearance, at more than a 95% confidence level.

Fatigue Test Results

Figure 9 shows the fatigue test results for 0.76-mm gauge laser beam welds

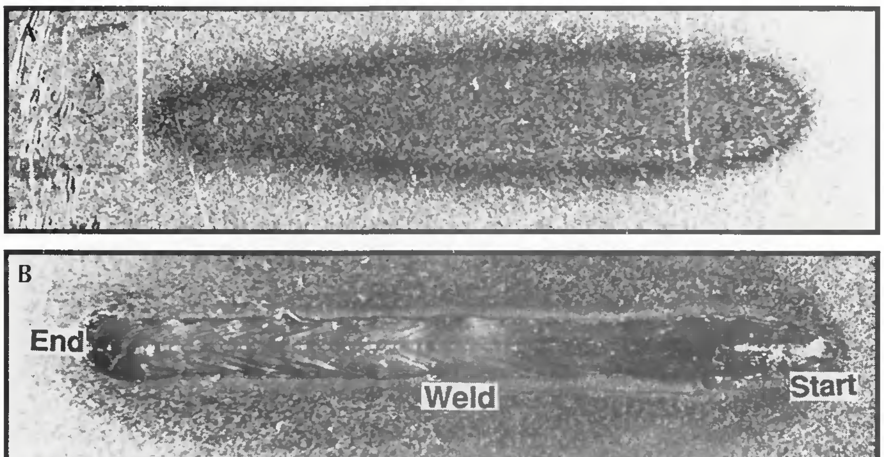

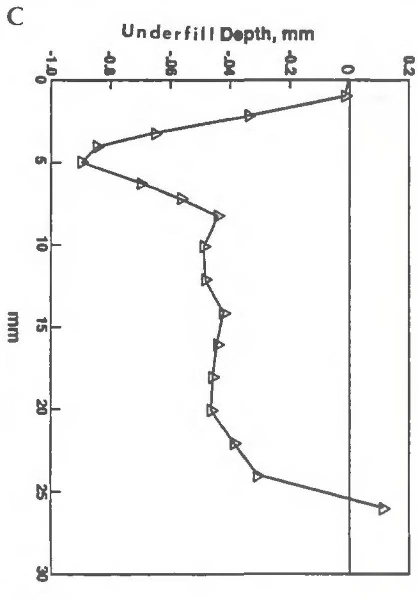

Fig. 7 — A — Photograph of bottom side of a 1.83-mm gauge laser beam weld with 50% underfill; B — photography of top side of a 1.83-mm gauge laser beam weld with 50% underfill; C — profile measurements of underfill.

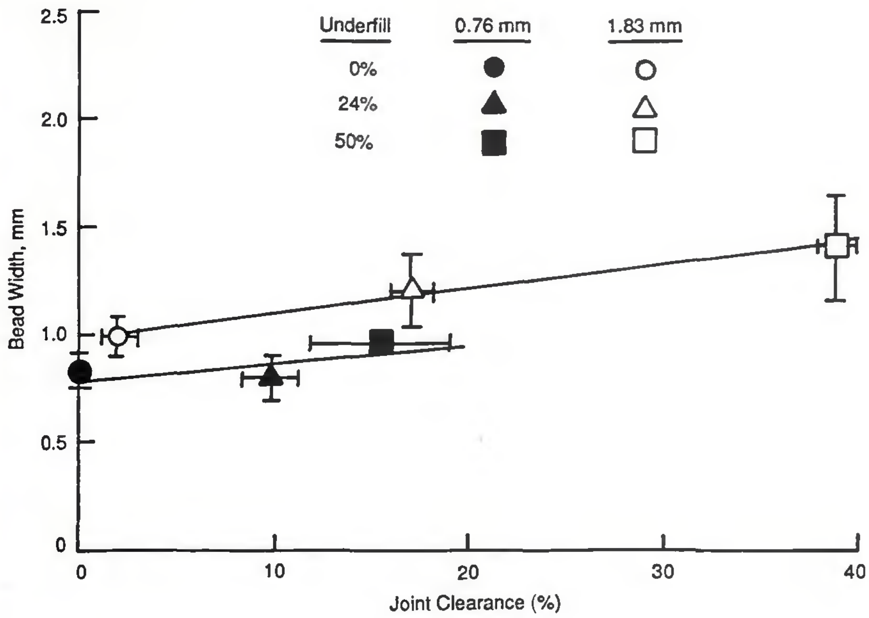

Fig. 8 — Bead width as a function of the joint clearance at the various underfills for 0.76-mm and 1.83-mm-gauge laser beam welds. The data for all underfills are included. The data points represent average values, while the error bars show the minimum and maximum values measured.

with 0% (Weld Z), 24% (Weld U) and 50% (Weld V) underfills, respectively. A regressional analysis was used to determine the load vs. life for each case. Comparing the test results of welds Z, U and V, we see the introduction of underfill decreases the fatigue life of a laser beam weld. However, different results were found for the case of 1.83 mm gauge laser beam welds. Figure 10 shows the fatigue test results for welds with 0% (Weld AA), 24% (Weld W) and 50% (Weld X) underfills. As shown, the welds with a 24% underfill gave the highest fatigue resistance, while the welds with a 50% underfill had the lowest fatigue resistance. The cause of the difference in fatigue resistance shown in Figs. 9 and 10 will be discussed in detail later.

Maddox (Ref. 13) studied fatigue cracks in fillet joints and found that if the negative inverse slope of load vs. life obtained by a regression analysis is close to the base material propagation constant m (shown in Paris's power law, $da/dN = C(\Delta K)^m$, where a is the crack length, N is the number of cycles, ΔK is the stress-intensity factor range, and C and m are the material constants (Refs. 14, 15)), then the fatigue is dominated by crack propagation. As shown in Fig. 9, the inverse slopes of regression line for welds Z, U and V are 5.02, 3.87 and 3.28, respectively. Abe, *et al.* (Ref. 16), performed an extensive study of the crack propagation rate of sheet steels and found that the value of m is approximately equal to 4 for mild steel. Comparing this value and the inverse slopes for these three welds suggests that the fatigue of laser beam welds is dominated by crack propagation. Similar results can be seen in Fig. 10 where the inverse slopes of regressional lines for welds AA, W and X are 4.57, 4.30 and 3.94, respectively. This deduction is consistent with the scanning electron micrographs reported in a previous study (Ref. 17).

Modeling

As mentioned in the introduction section, a difficulty in assessing the effects of weld discontinuities on fatigue performance is how underfill, joint clearance and bead width are interrelated. Here we use the aforementioned fatigue model and a statistical analysis method to separate the individual effects of these three on fatigue resistance of the laser beam welds. As shown in Fig. 1, a specimen is made of two steel coupons with a bead width (bW), joint clearance (G) and underfill (U). A 2^3 factorial design was used in this study. That is, two levels were chosen for each of the three variables ("factor"), and fatigue life calculations were performed for all combinations (Ref. 18).

In order to analyze the calculated results from using a fatigue model, a linear relationship is assumed between fatigue life and the variables (bW, G and U). Both "main" and "interactive" effects are combined to form the linear model used in the analysis of the calculated fatigue lives obtained in this study:

$$N_f = c_1 + c_2 \cdot bW + c_3 \cdot G + c_4 \cdot U + c_5 \cdot bW \cdot G + c_6 \cdot bW \cdot U + c_7 \cdot G \cdot U + c_8 \cdot bW \cdot G \cdot U \quad (5)$$

In Equation 5, N_f is the calculated fatigue life for a particular set of the variables. The coefficients c_2, c_3, ...c_8 are the estimated effects of (bW), (G),....(bW) (G) (U), respectively.

Fatigue life for a specific set of weld geometries under a given load can be calculated using Equation 2. The values of c_1, c_2, c_8 can be determined by solving the simultaneous mathematical equations after inserting the fatigue life N_f into Equation 5.

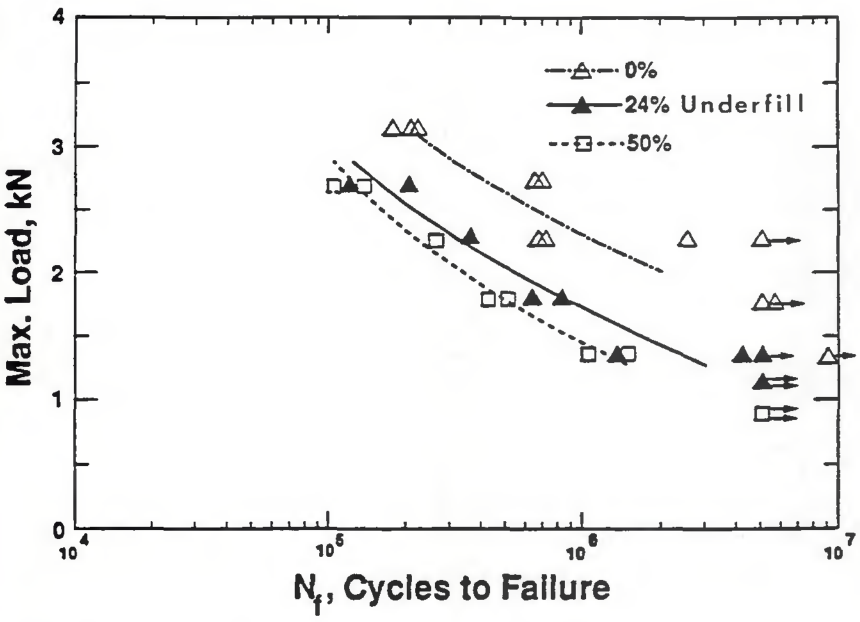

Fig. 9 — Effect of underfill on fatigue resistance of 0.76-mm-gauge laser beam welds.

Discussion

Effect of Weld Discontinuities

The statistical analysis described above was applied to examine the effects of bead width (bW), joint clearance (G) and underfill (U). For practical purposes, a range of dimensions for bead width, joint clearance and underfill typically found on the prototype components were investigated. The welds were made on two steel coupons with an overlap length of 38.1 mm (1.5 in.) and a sheet width of 38.1 mm. The specific values chosen were bW = 0.8 mm (0.031 in.) and 2.4 mm (0.094 in.), G = 2 and 25%, and U = 0 and 50%. The eight weld geometry cases are listed in Table 3. A load of 2.1 kN (470 lb) with a load ratio R = 0 (R = min/max load) was applied to the welds. Individual effects of the above three variables on fatigue life are discussed in detail below.

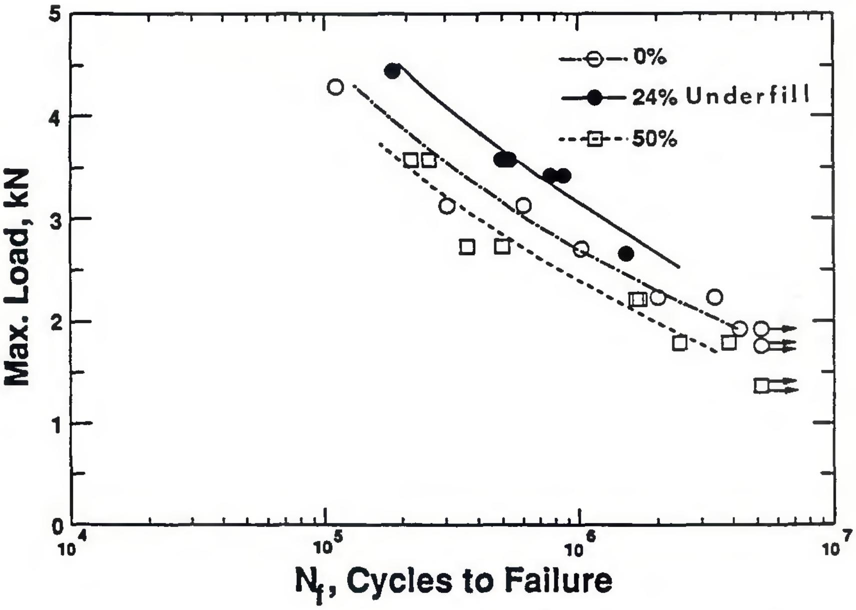

Fig. 10 — Effect of underfill on fatigue resistance of 1.83-mm gauge laser beam welds.

Bead Width

The main and interactive effects of the two levels of bead width (bW), joint clearance (G) and underfill (U) on fatigue life of 0.76- and 1.83-mm-gauge laser beam welds are shown in Table 4. It should be recognized that the fatigue life for a specific case of bead width (bW = 0.8 or 2.4 mm) is given by inserting the bead width value into Equation 5 and using the appropriate coefficients from Table 4. Figure 11 shows the calculated effect of bead width on fatigue life of laser beam welds with U = 0%, and with G = 2 and 25%. As shown, fatigue life is found to be very sensitive to bead width. An increase in bead width resulted in a substantial increase in fatigue life. Furthermore, there is an interaction between bead width and joint clearance. The lines drawn between bW = 0.8 mm and bW = 2.4 mm for each joint clearance are not parallel (as it would be if there were no (bW)(G) interaction). For larger bead width, there is a greater increase in fatigue life with decreasing joint clearance. The increase in fatigue life due to an increase of bead width is more pronounced for the case of 0.76-mm-gauge laser beam welds.

Joint Clearance

Figure 12 shows the effect of joint clearance (G) on fatigue life of laser beam welds with bW = 1.2 mm, and with U = 0 and 50%. Increasing the joint clearance results in a decrease in fatigue life. This reduction in fatigue life is attributed to the high geometric stress riser introduced at the intersection of the weld bead and opening of the sheets. As shown in Fig. 12, for 0.76-mm-gauge specimens, underfill does not interact with joint clearance, but there is a slight interaction for the case of 1.83-mm-gauge specimens. Specifically, the specimens having the larger underfill show a greater decrease in fatigue life when the joint clearance is increased. The decrease in fatigue life due to an increase of joint clearance is more pronounced for the 0.76-mm-gauge specimens. A comparison of Figs. 11 and 12 reveals that the degree of life change caused by altering joint clearance is not as great as the bead width effect.

Underfill

The effect of underfill on fatigue life of laser beam welds with bW = 1.2 mm, and with G = 10% is shown in Fig. 13. It is seen that as the underfill increases, fatigue life decreases. The decrease in fatigue life is more pronounced for thicker gauge specimens. Within the selected range of bead width and joint clearance studied here, the degree of life change caused by altering underfill is not as great as the effects of bead width and joint clearance.

The analyses conducted above assume a linear relationship between fatigue life and the underfill, joint clearance and bead width. In reality, this may

Table 3 — Range of Variables for Statistical Analysis

Case	Bead Width (mm)	Joint Clearance (%)	Underfill (%)
1	0.8	2.0	0.0
2	0.8	2.0	50.0
3	0.8	25.0	0.0
4	0.8	25.0	50.0
5	2.4	2.0	0.0
6	2.4	2.0	50.0
7	2.4	25.0	0.0
8	2.4	25.0	50.0

Table 4 — Calculated Effects of Bead Width, Joint Clearance and Underfill on Fatigue Life of Laser Beam Welds

Effect	Coefficient	Sheet Thickness 0.76 mm Calculated (cycles)	Sheet Thickness 1.83 mm Calculated (cycles)
Mean	c_1	-1.55×10^6	-1.07×10^7
bW	c_2	2.12×10^6	1.51×10^7
G	c_3	1.70×10^6	1.10×10^7
U	c_4	2.29×10^5	2.38×10^6
(bW) (G)	c_5	-2.26×10^6	-1.18×10^7
(bW) (U)	c_6	-2.98×10^5	-3.89×10^6
(G) (U)	c_7	1.82×10^4	2.87×10^6
(bW) (G) (U)	c_8	-5.34×10^3	-6.02×10^6

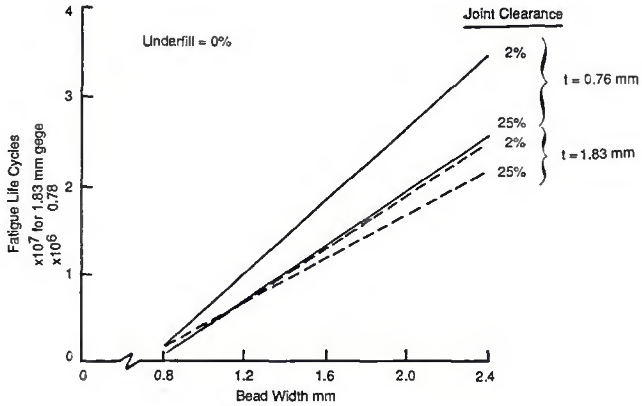

Fig. 11 — The predicted effect of bead width on fatigue life of a laser beam weld.

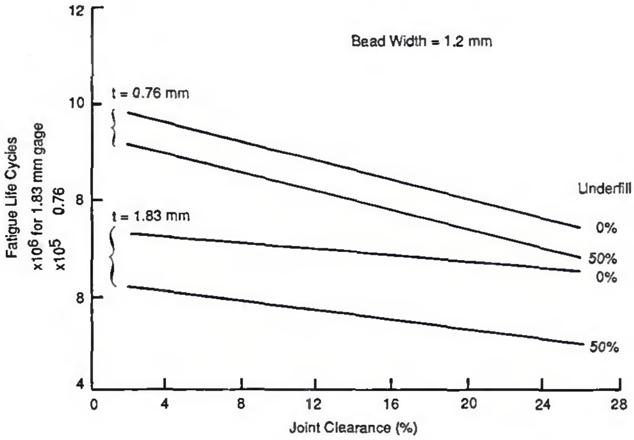

Fig. 12 — The predicted effect of joint clearance on fatigue life of a laser beam weld.

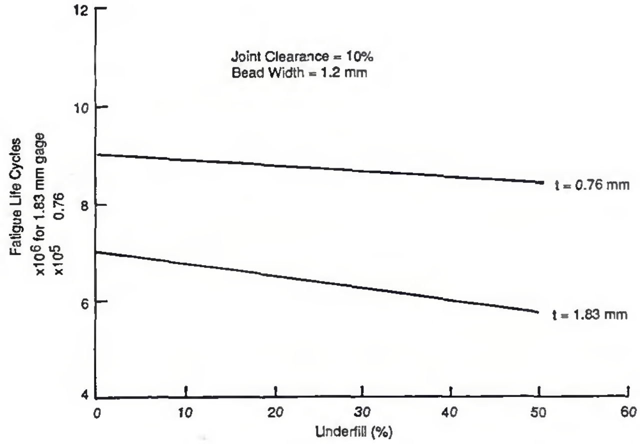

Fig. 13 — The predicted effect of underfill on fatigue life of a laser beam weld.

not be the case, and a high order relationship may be needed for better analyses. However, since the dimension range studied here is fairly narrow, we think that, to a first order approximation, the use of a linear relationship is justified.

The Combined Effect of Bead Width, Joint Clearance and Underfill

Based on the above discussions, the fatigue life is mainly determined by the balance of the negative changes in joint clearance and underfill against the positive effect of the bead width. As shown in Fig. 8, for the case of 0.76-mm-gauge specimens, the joint clearance increases with increasing the underfill from 0 to 24%, while the bead width varies little. Modeling results showed that increasing joint clearance led to an increase in stress concentration at the periphery of the weld bead, and consequently, resulted in a decrease in fatigue resistance, which is consistent with the test results shown in Fig. 9. An increase in underfill from 24 to 50% resulted in an increase in both joint clearance and bead width. Modeling results showed that fatigue strength decrease due to the increase in joint clearance and underfill is compensated by the gain from the increase in bead width. As a result of this, the combined effect of underfill, joint clearance and bead width reduces the fatigue strength for specimens with 50% underfill only slightly more than that for specimens with 24% underfill, which is in agreement with experimental results shown in Fig. 9.

For the case of 1.83-mm-gauge specimens, bead width and joint clearance both increase with increasing weld underfill — Fig. 8. Modeling results showed that, under a load of 2.1 kN (470 lb), as the underfill increased from 0 to 24%, fatigue life decreased from 4.2 X 10^6 cycles to 3.86 X 10^6 cycles. An additional decrease in life from 3.86 X 10^6 to 3.65 X 10^6 cycles was predicted with the change in joint clearance from 1.6 to 16%. An increase in life from 3.65 X 10^6 to 6.18 X 10^6 cycles was estimated with the increase in magnitude of bead width from 0.99 to 1.2 mm. As a result, welds with 24% underfill gave a higher fatigue resistance. A comparison of predictions with the experimental results shown in Fig. 10 indicates that the model gives good predictions. Comparing the welds with 0 and 50% underfills, calculations show that the life loss due to increase in joint clearance and underfill outweighs the life gain due to the increases in bead width. As a result, welds with a 50% underfill had the lowest fatigue life. Thus, it appears that there is an optimum combination of underfill, bead width and joint clearance for each specific gauge laser beam weld that gives the highest fatigue resistance.

The present investigation clearly demonstrated the usefulness of the computational model, which can provide designers with a tool for assessing the effects of weld discontinuities on fatigue resistance of laser beam welds. However, the results and fatigue model presented here are only for transverse laser beam welds, whereas, laser-welded vehicle components are designed with various weld orientations. Since the analyses agree with experimental results, we believe that the same approach can be used for the longitudinal laser beam weld (*i.e.*, weld is parallel to loading direction).

Conclusions

The effects of weld discontinuities on the fatigue life of laser beam welds have been investigated. The following conclusions can be drawn:

1) Bead width (root penetration) has a strong influence on the fatigue life of a laser beam weld, with life increasing as the bead width increases (good root penetration).

2) An increase in the joint clearance between sheets would result in a significant decrease in fatigue life. The degree of life change is smaller than the bead width effect.

3) The presence of underfill decreases the fatigue life. The decrease in fatigue life is more pronounced as the sheet gauge is increased. The degree of life change is not as great as the effects of bead width and joint clearance.

4) The fatigue life of a laser beam weld is determined by a balance between the effects of joint clearance, underfill and root penetration. As a result, there is an optimum fatigue strength for each specific gauge laser beam weld.

5) Fatigue of a laser beam weld is dominated by crack propagation.

Acknowledgment

The author wishes to thank M. N. Uddin, formerly with General Motors Corp., of Thyssen Steel Technical Center for conducting the fatigue testing.

References

1. Hyder, A., Uddin, M. N., and Speranza, J. 1989. Unpublished work, Chevrolet-Pontiac-Canada *Manufacturing Engineering*, General Motors Corp.
2. ANSI/AWS A3.0-89, *Standard Welding Terms and Definitions.*
3. Kan, Y. R. 1976. Fatigue resistance of spot welds — an analytical study. Metals Eng. Quarterly, pp. 26–36.
4. Oh, L. H., 1982. Fatigue-life prediction for spot weld using Neuber's rule. ASTM STP 761 pp. 296–309.
5. Swellam, M. H., Kurath, P., and Lawrence, F. V., Jr. 1991. Electric-potential-drop studies of fatigue crack development in tensile-shear spot welds. ASTM STP 1122.
6. Wang, P. C., and Ewing, K. M. 1988. A J-Integral approach to fatigue resistance of a tensile-shear spot weld. SAE Paper 880373.
7. Wang, P. C., and Ewing, K. M. 1991. Fracture mechanics analysis of fatigue resistance of spot welded coach-peel joints. *Fatigue Fract. Eng. Mater. Struct.* Vol. 14, No. 9, pp. 915–930.
8. Pook, L. P. 1975. Fracture mechanics analysis of the fatigue behavior of spot welds. *Int. J. of Fracture*, 11, pp.173–176.
9. Rice, J. R. 1968. J. Appl. Mechanics, Trans. 35, 379–386.
10. Barsoum, R. S. 1976. On the use of isoparametric finite elements in linear fracture mechanics. *Int. J. for Numerical Methods in Eng.* 10: 25–37.
11. *ABAQUS User's Manual.* Hibbitt, Karlsson and Sorensen, Inc., Providence, R.I.
12. Dowdy, S., and Wearden, S. 1983. *Statistics for Research.* John Wiley & Sons, New York, N.Y., p. 185.
13. Maddox S. J. 1970. Fracture mechanics applied to fatigue in welded structure. British Welding Inst. Report No. E/36/70.
14. Paris, P. C., Gomez, M. P., and Anderson, W. E. 1961. A rational analytical theory of fatigue. *The Trend in Engineering*, 13: 9–14, University of Washington.
15. Paris, P. C. 1964. The fracture mechanics approach to fatigue, fatigue — an interdisciplinary approach. Proc. 10th Sagamore Army Materials Research Conf. eds. J. J. Burke, N. L. Reed and V. Wiess, pp. 121–134, Syracuse Univ. Press.
16. Abe, H., Kataoka, S., and Satoh, T. 1986. Empirical formula for fatigue strength of single-welded joint specimens under tensile-shear repeated load. SAE Paper 860606.
17. Wang, P. C., and Ewing, K. M. 1991. A comparison of fatigue strengths: laser beam vs. resistance spot welds. *Welding Journal* 70(10): 43–47.
18. Box, G., Hunter, W., and Hunter, J. 1978. *Statistics for Experiments.* p. 306, New York, N.Y., Wiley.

WRC Bulletin 364
June 1991

This bulletin contains two reports:

(1) New Design Curves for Torispherical Heads

By A. Kalnins and D. P. Updike

(2) Elastic-Plastic Analysis of Shells of Revolution under Axisymmetric Loading

By D. P. Updike and A. Kalnins

Publication of these reports was sponsored by the Committee on Shells and Ligaments of the Pressure Vessel Research Council. The price of WRC Bulletin 364 is $40.00 per copy, plus $5.00 for U.S. and $10.00 for overseas, postage and handling. Orders should be sent with payment to the Welding Research Council, Room 1301, 345 E. 47th St., New York, NY 10017.

WRC Bulletin 366
August 1991

Recommended Practices in Elevated Temperature Design: A Compendium of Breeder Reactor Experiences (1970–1987), Volume IV — Special Topics

Edited by A. K. Dhalla

The recommended practices for elevated temperature design of Liquid Metal Fast Breeder Reactors (LMFBR) has been consolidated into four volumes and is published in four individual WRC Bulletins.

Volume I — Current Status and Future Directions, in WRC Bulletin 362, April 1991
Volume II — Preliminary Design and Simplified Methods, in WRC Bulletin 363, May 1991
Volume III — Inelastic Analysis, in WRC Bulletin 365, July 1991
Volume IV — Special Topics, in WRC Bulletin 366, August 1991

In Volume IV, WRC Bulletin 366, special topics such as, fracture mechanics, nonlinear collapse stress classification of structural discontinuity stresses, and high temperature design as practiced in Germany are discussed. Flaw evaluation (fracture mechanics) procedures are recommended to supplement the design codes which assume perfect, defect-free structures. The fracture mechanics methods have been extended into the plastic and creep regimes.

Publication of this Bulletin was sponsored by the Committee on Elevated Temperature of the Pressure Vessel Research Council. The price of WRC Bulletin 366 is $40.00 per copy, plus $5.00 for U.S. and $10.00 for overseas, postage and handling. Orders should be sent with payment to the Welding Research Council, Room 1301, 345 E. 47th St., New York, NY 10017.